

Measurement of the time resolution of the installed muon chambers with the 2008 cosmic runs



LHCb Public Note

Issue: 1
Revision: 3
Reference: LHCb-PUB-2009-016
Created: May 22, 2009
Last modified: Sep 17, 2009

Prepared by: W. Bonivento, F. Dettori, G. Manca, R. Oldeman, M. Sireus,
Università and INFN, Sezione di Cagliari, Italy, G. Graziani, G. Passaleva, INFN, Sezione di
Firenze, Italy

LHCb-PUB-2009-016
17/09/2009



Abstract

One of the main goals of the LHCb muon system commissioning is to assess the detector performance and identify possible misbehaviors in the installed chambers: this is partially possible using cosmic ray muons tracked through the detector.

In this note we focus on the measurement of the time resolution of the whole installed detector (M2-M5 stations) using the 2008 commissioning data. Results are compared with the expected performances.

Contents

1	Introduction	1
2	Data sample, track and time reconstruction	2
3	Expectations	2
4	Hardware related issues	3
4.1	Nonlinearities of the TDC	3
4.2	Pathological channels	4
5	Time alignment	4
5.1	Internal time alignment	4
5.2	Using calorimeter	5
5.3	Comparison	9
6	Time resolution from the cosmic data	9
6.1	Method to extract the time resolution	9
6.2	Results	11
6.3	Systematics	12
7	Conclusions	14
8	References	15

1 Introduction

One of the main goals of the commissioning of the LHCb detectors is to compare their performance in the pit with the one obtained during beam and laboratory tests.

For the muon system [1], there are few important chamber parameters to be checked, such as the efficiency, the time resolution, the logical pad cluster size, the noise, the number of dead channels and shorts.

In order to obtain the design efficiency, the most stringent requirement for the muon chambers is the ability to reconstruct the signal in all four M2–M5 stations within the 25 ns gate around each bunch crossing.

This note deals with the measurement of the time resolution of the installed muon chambers using cosmic rays acquired during the 2008 commissioning.

Section 2 describes the data sample and the reconstruction criteria.

In section 3 we remind the differences with the laboratory tests and we discuss the expectations for the performance in the pit.

In section 4 we review the hardware problems that were encountered during the commissioning and must be

taken into account for this analysis.

In section 5 we discuss the time alignment procedure performed using only muon chambers or with the help of the calorimeter.

In section 6 we present the results of the time resolution measurement, after discussing the method and its validation.

In section 7 we draw conclusions.

2 Data sample, track and time reconstruction

In this analysis we use cosmic data acquired using calorimeter trigger during three nights in september/october 2008. The whole installed muon detector (M2–M5 stations) was read out. High voltage was set to 2500 V on all chambers and no CF₄ was present in the gas mixture^a. The thresholds were set at 10.5 fC on M4R3 and M5R3, and 7.5 fC on the other regions with pad readout; 18fC on M4R4 and M5R4, and 15fC on the other regions with wire readout. This corresponds to a factor 1.5 higher than the nominal values.

The data sample consists of 1.4 millions triggered events. Seven consecutive bunch crossings around the triggered one were acquired, in order to have a time gate of $7 \times 25 = 175$ ns, large enough to include possibly time-misaligned signals.

Track reconstruction uses an algorithm based on a Hopfield recurrent neural network [2], developed for the online monitoring in order to discriminate cosmic tracks from noise hits efficiently. Tracks were reconstructed requiring at least three aligned hits in different stations. Firing hits adjacent to the initial seeds are also attached to the track, and a fit quality cut $\chi^2/dof < 1.7$ is applied in both xz and yz views.

About 380k tracks were reconstructed with hits in at least 3 stations, 120k of which have hits in all 4 stations.

The chamber response time is obtained for each logical pad associated to the track from the BX counter and the 4 bit TDC measuring the fine time of each logical channel in the ODEs. For regions with double readout (M23R12) we consider the X and Y time measurements as independent and we will estimate the time resolution separately for the two views. For the pads obtained by crossing two logical channels triggered by the same physical channel (M23R34 and M45R234), we average the two measurements, that are expected to agree within the jitter of the readout chain (~ 1 ns).

In order to suppress the combinatorial background from the crossing of two unrelated logical channel hits, we require the two measurements to agree within 2 TDC bins (3.1 ns) for regions with single readout, and within 25 TDC bins (39 ns, more than 5 times the expected resolution) for regions with double readout. The presence of such background can be inferred from the tails in the distribution of the time difference shown in fig. 1 and is probably enhanced by the presence of some masked logical channels (see sec. 4).

3 Expectations

Measurements performed on a few chambers in a test stand using cosmic rays [3] are well suited for a comparison with our analysis. The effect of threshold t and high voltage V on the chamber gain G was shown to follow the following laws:

$$G \propto \frac{1}{t}$$

$$G \propto \exp\left(\frac{V}{152V}\right) \quad (1)$$

Thus, the time resolution for the values of high voltage V_{pit} and threshold t_{pit} is expected to be equal to the one measured on the test stand at high voltage

$$V_{eq} = V_{pit} + 152V \times \ln\left(\frac{t_{lab}}{t_{pit}}\right) \quad (2)$$

^athe nominal gas mixture is Ar/CO₂/CF₄ in proportions 40/55/5

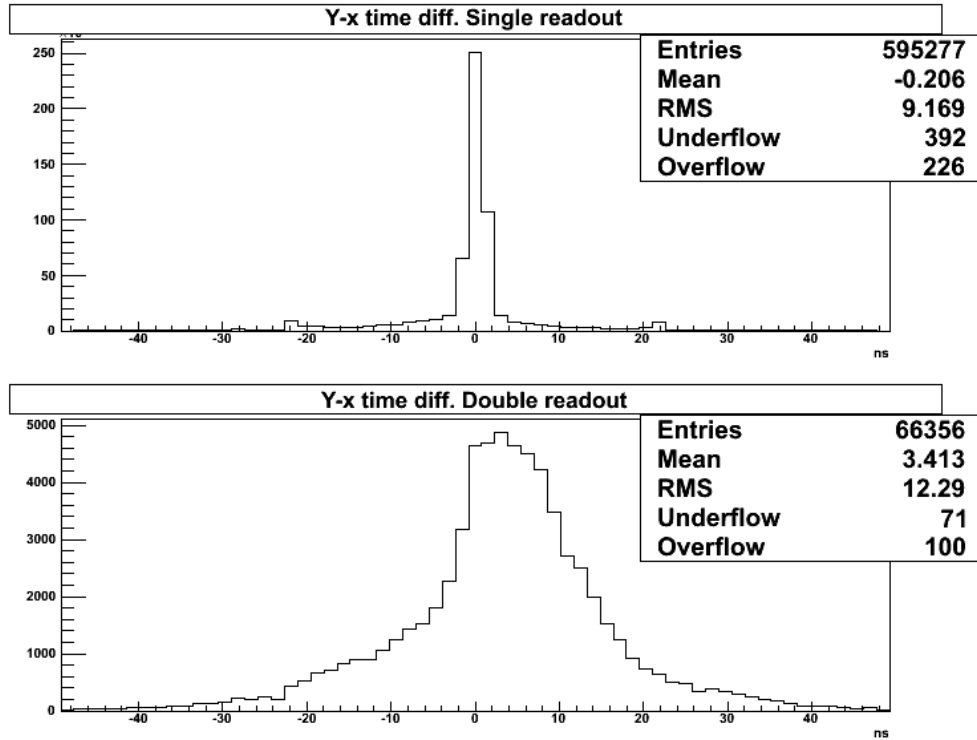


Figure 1 Difference between the raw time in y and x views for pads obtained by crossing two logical channels, for regions with single readout (top plot) and double readout (bottom plot).

were t_{lab} is the threshold value used in the test stand measurement.

Moreover, we need to consider that the absence of CF_4 in the gas mixture is equivalent to a 10 V drop of the high voltage [4]).

The results of this calculation are shown in table 1.

Uncertainties on the expected resolution values, coming from the (unknown) difference between pressure, temperature and individual chamber to chamber variation of gap gain, can be estimated to be ± 50 V in the equivalent H.V. values, corresponding to ± 1.0 ns on the resolution.

Table 1 Threshold settings of pit 2008 and laboratory tests, and expected time resolutions for different regions. From first to last column, the chamber type, the threshold values t_{pit} and t_{lab} , the equivalent HV values V_{eq} and the measured time resolution at V_{eq} .

chamber	t_{pit} (fC)	t_{lab} (fC)	V_{eq} (V)	σ_t (ns)
M5R4	18	10	2400	6.8
M5R3	10.5	7	2430	6.1
M3R3	7.5	5	2430	5.2
M4R2	7.5	5	2430	5.5

4 Hardware related issues

4.1 Nonlinearities of the TDC

The TDC circuit of the SYNC chip was found to have a non linear behavior, which is at present well understood. The main effect is a time response distortion in the last and (to a lesser extent) first two of the 16 bins of the 4

bit TDC range. This prevents an accurate time measurement when the signal time is close to the borders of the triggered BX, while the TDC output is still reliable when the signal is well aligned with the trigger (the “normal” situation during the physics run).

To limit the impact of this effect, signals recorded in the last two bins were not used to measure the time resolution. This introduces a systematic effect on the resolution that will be estimated in section 6.3.

4.2 Pathological channels

The acquisition of cosmic rays was performed in parallel with the debugging activity on the freshly installed detectors, and some channels showing problems under investigation had to be excluded from the analysis. About 6% of the logical channels were masked at FE or ODE level due to noise, connectivity or timing problems. Other 0.5% of channels showed high noise level and were masked offline to avoid a bias on the results from ghost tracks.

At the time of writing, most of these hardware problems were investigated and fixed.

An incorrect behaviour in the time response was noticed in the last three (out of 12) trigger sectors of all ODEs for regions M4/5 R3/4, where the time difference between the x and y measurements showed typical values much higher than the expected electronic jitter (in these region the x and y logical channels come from the same physical channel).

The reason was traced back to a cable inversion, that was fixed after the data were taken. The concerned 480 logical channels (2.9% of the total) were removed from this analysis.

5 Time alignment

During the commissioning a partial hardware time alignment of the logical channels was performed:

- all channels were time aligned, with an accuracy of about 1 ns, with respect to a pulser module (PDM);
- a per station correction was applied to compensate the time of flight of forward tracks parallel to the beam direction (about 4 ns between two consecutive stations), in order to provide a reasonable alignment for forward tracks to the muon trigger.

In order to fully exploit the time performance of the apparatus, the time alignment must be refined to account for the delays and cable lengths of the pulser chain and the real signal time shape. The residual effects are expected to be of the order of several ns. This requires the use of physical signals from real tracks. Though a satisfactory alignment, especially for the inner regions, will be obtained only from the first physics beam, the collected statistics of cosmic tracks allows for a software offline procedure, aiming at removing the contribution of the residual misalignment from the measured time resolution.

Two different time alignment strategies were used.

5.1 Internal time alignment

We evaluate the misalignment for every channel c with respect to the other channels on the same track, by averaging the residual

$$r_c = \left(t_c - \frac{\sum_{i=1}^n t_i}{n} \right) \quad (3)$$

over all tracks containing channel c . Here t is the time corrected for the time of flight, computed for each track according to its fitted trajectory.

Each channel corresponds to a logical pad, except for regions with double readout (M23R12) where X and Y views are considered as two different channels. We compute for each channel a correction

$$\Delta T_c = -\alpha \langle r_c \rangle \quad (4)$$

and we iterate the procedure ($\alpha = 0.8$ is a factor to damp possible oscillations) until the number of significant corrections becomes negligible.

This procedure is limited by statistics. Though the average number of tracks per channel is 18.6, the value is much smaller for inner regions, as shown in figure 3. To avoid overperforming the alignment (we're using the same data from which we'll estimate the resolution) we apply the correction only if its statistical error $\sigma(\Delta T_c)$ is smaller than 1 ns, or if $\Delta T_c/\sigma(\Delta T_c) > 1.5$ (where $\sigma(\Delta T_c)$ is conservatively estimated as $7 \text{ ns}/\sqrt{n_c}$, where n_c is the number of tracks containing channel c).

After five iterations the procedure converges (see fig. 4). Figure 5 shows the geometrical map of the time misalignment.

We obtain significant time shifts for 53% of the active channels, covering 78% of the data for this analysis. The distribution of the applied corrections is shown in fig. 2. The r.m.s of 6 ns gives an indication of the expected contribution of time misalignment to the detector time resolution (before alignment correction).

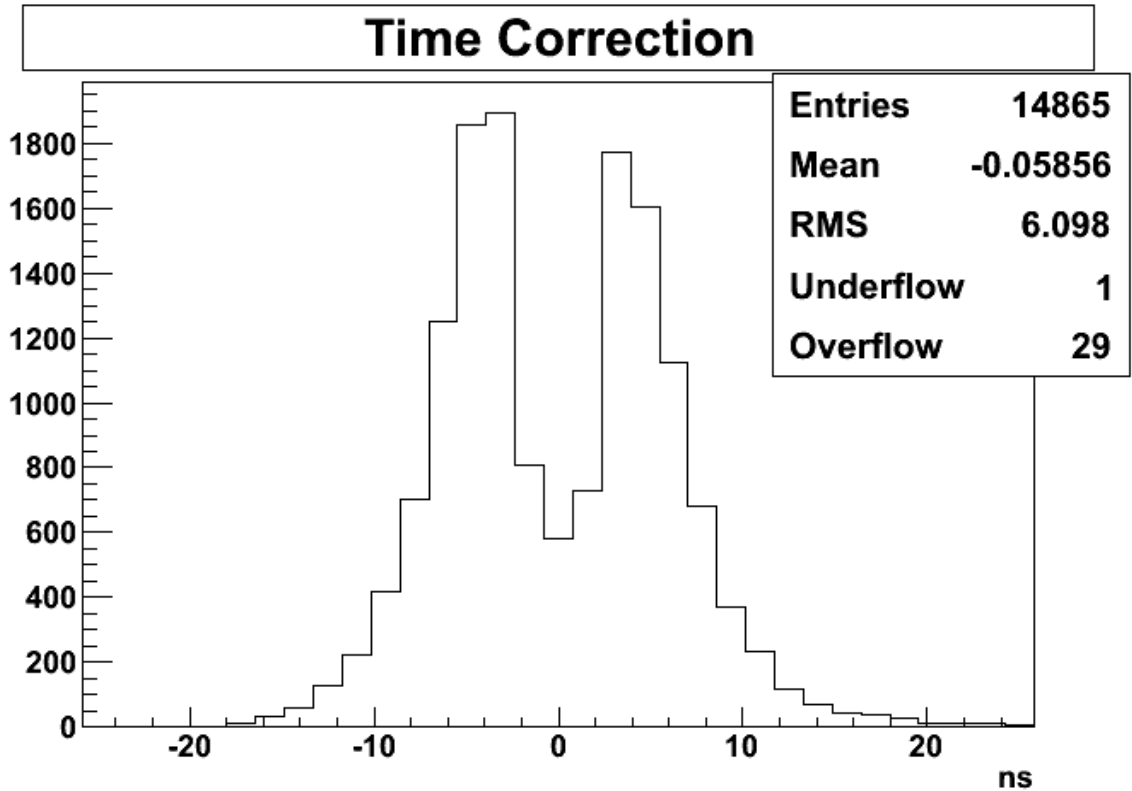


Figure 2 Distributions of the significant time shifts obtained with the internal alignment procedure.

The average error on the applied time shifts is 1.2 ns. The overtraining is expected to produce an underestimation of the resolution of this order (to be added in quadrature). On the other hand, we expect a systematic overestimation from the channels that can't be corrected due to the limited statistics.

5.2 Using calorimeter

Another alignment procedure has been developed independently. The principal differences are:

- the trigger is used as a reference time. This procedure allows for an absolute calibration of the muon system, i.e. an average time offset with respect to the trigger can also be corrected. On the other hand, the misalignments in the calorimeter and calorimeter trigger systems enter into the muon system^b;
- the channels are grouped to reduce the statistical uncertainty on the alignment parameters;

^bThe time alignment between the calorimeter and muon systems was studied in detail [5] and showed to be satisfactory, except for a possible systematic shift of about 3 ns between region 4 and the other regions.

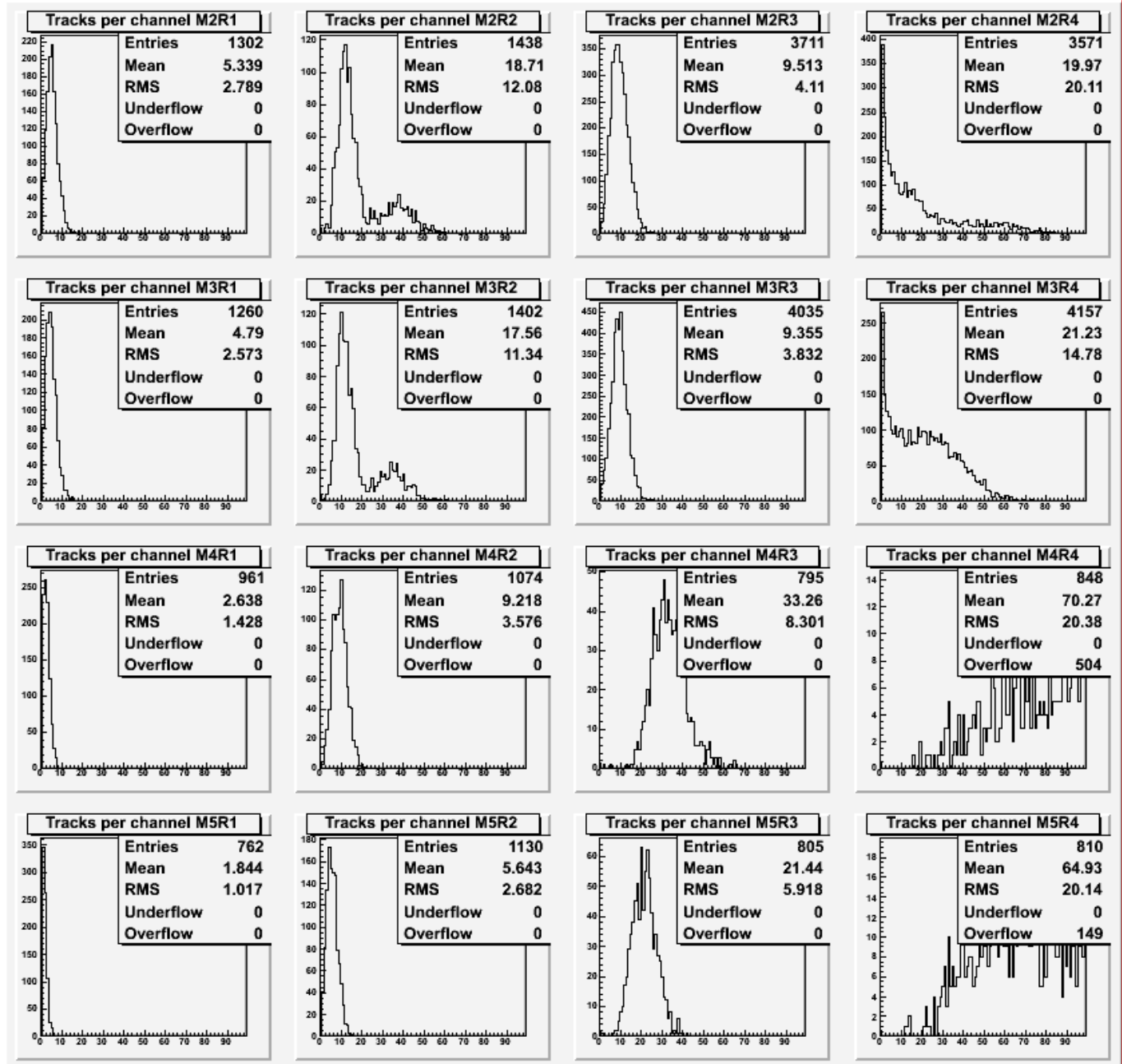


Figure 3 Average number of tracks per channel in different regions.

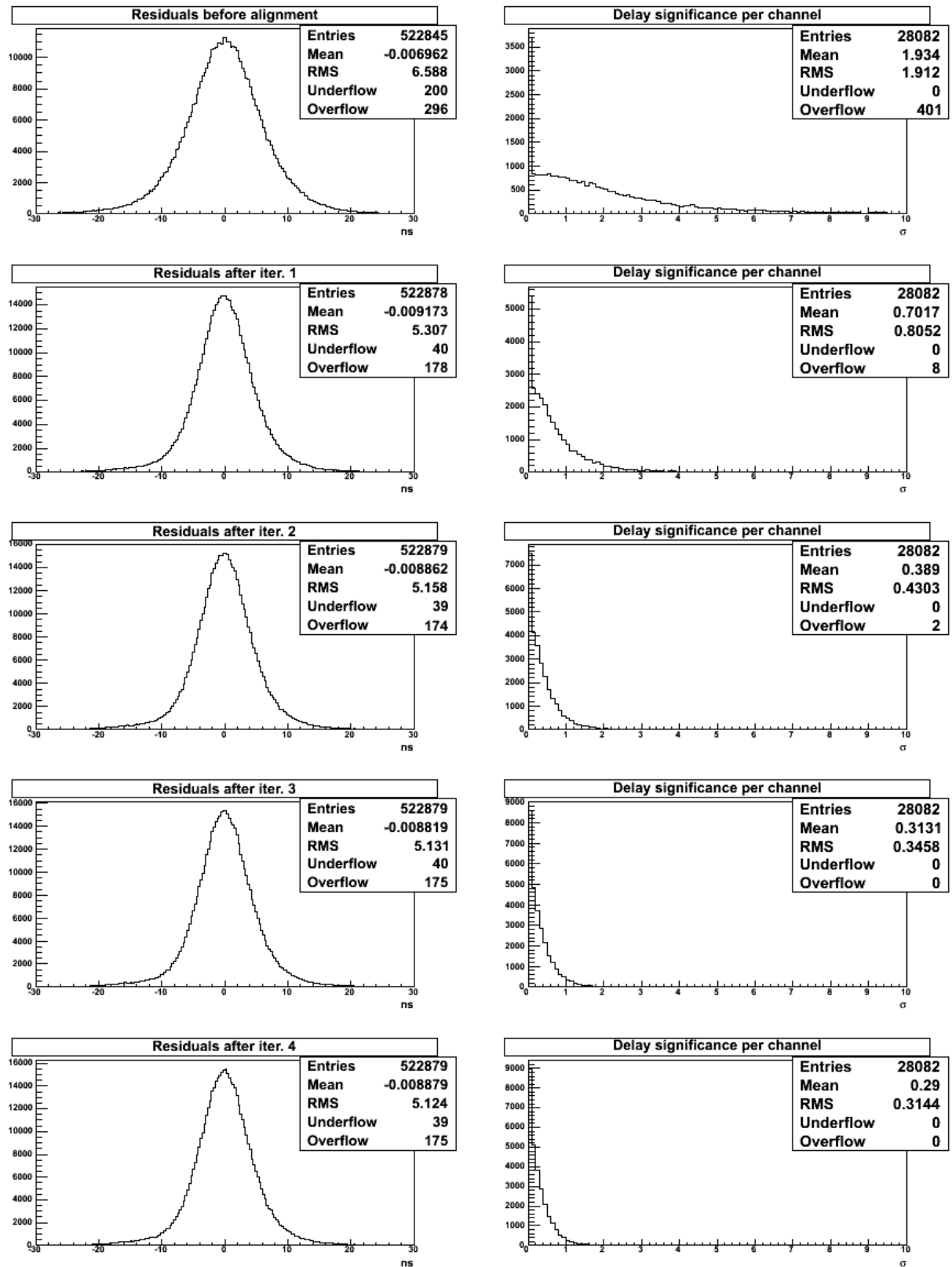


Figure 4 Distributions of residuals (left) and of the applied time shifts (right plots, divided by their errors) after the iterations of the internal alignment procedure.

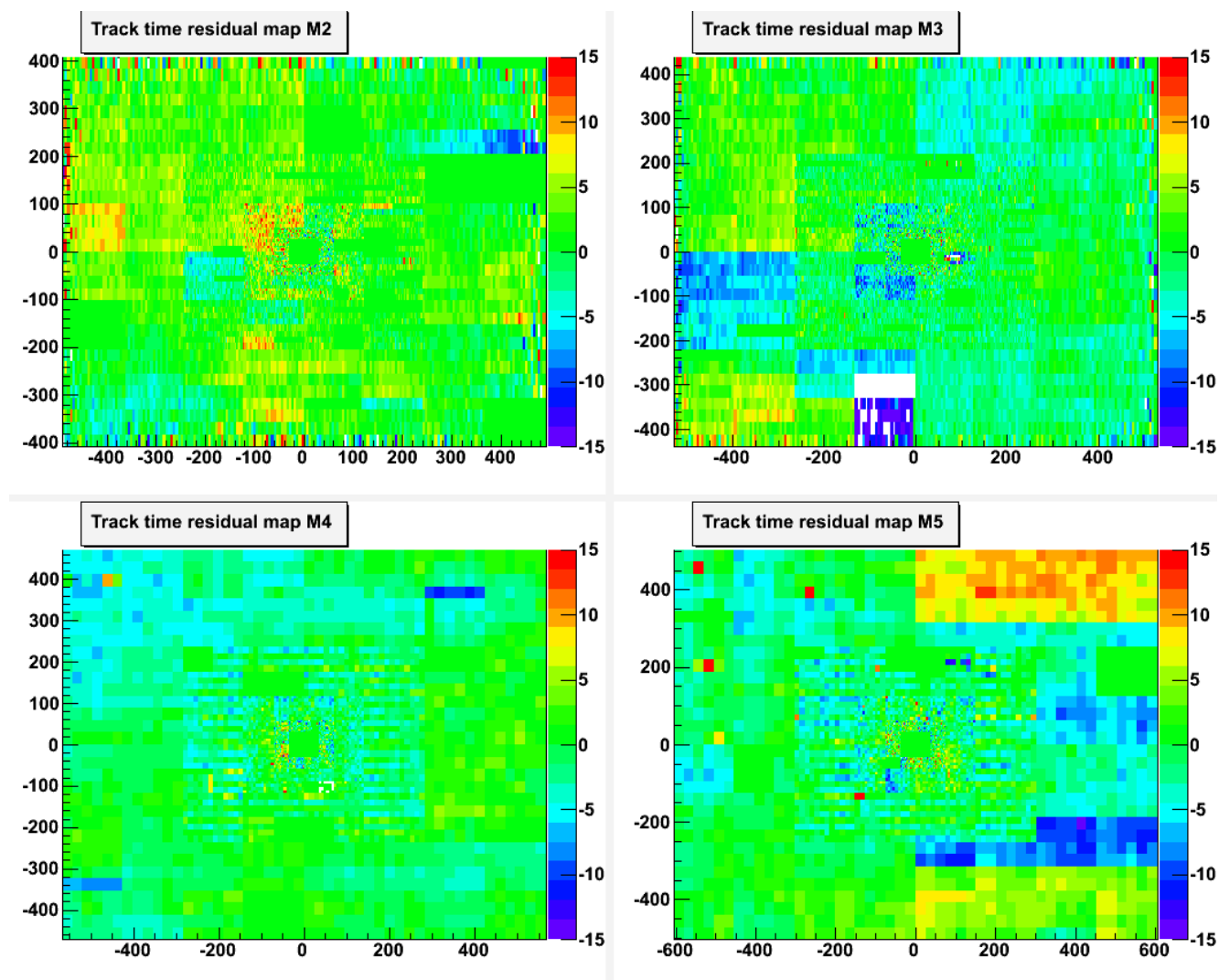


Figure 5 Map of the average time residual (on the z axis, in ns) for each logical pad of the M2–M5 stations. The X and Y coordinates are expressed in cm. Patterns related to channels on the same SYNC, ODE or chamber are clearly visible.

- an alternative track reconstruction method is used, using a combinatorial algorithm, described in detail in [6].

The grouping of channels was chosen to achieve a statistical uncertainty of less than 0.5 TDC bin, meaning that for 95% of the channels the statistical uncertainty is less than 1 bin. For an approximate time resolution of 5 TDC bins, this corresponds to an average of 100 time measurements. Since the illumination of the detector is not uniform, some groups receive less than the average, and the actual minimum number of time measurements to produce an alignment constant was set to 20. Table 2 lists the size of the groups in terms of logical pads.

Table 2 Grouping of logical pads for the “calo” time alignment

region	M2/M3	M4/M5
1	48x4	12x4
2	24x2	6x2
3	12x1	3x1
4	4x1	1x1

For each group, the average time is determined, and the difference with the central value, 7.5 TDC bin, is used as the alignment constant for all channels in the group.

5.3 Comparison

We compare the results from the two alignment methods in fig. 6 for the 14865 channels for which both procedures could be applied. A good agreement is found, the correlation factor between the two sets of corrections being 83%.

6 Time resolution from the cosmic data

6.1 Method to extract the time resolution

The time resolution was extracted from the cosmic data taken at the pit as follows. If we consider each of the n time measurements t_i in a given track as a sampling of a random variable with variance σ^2 , the sample variance

$$s^2 = \frac{\sum_{i=1}^n (\bar{t} - t_i)^2}{n - 1} \quad (5)$$

is a correct estimator of σ^2 . Though the average number of measurements per track n is low, the average of s^2 over the large number of tracks allows for a precise measurement. Figure 7 shows the distributions for n and s^2 .

If we take into account that the resolution depends on the region, s^2 will estimate the average variance. To estimate the resolution for a given region σ_R , we consider only the tracks with a hit in that region t_R . The average variance for these tracks will be

$$\sigma^2 = \frac{\sigma_R^2 + (n - 1)\sigma_{\bar{R}}^2}{n} \quad (6)$$

where $\sigma_{\bar{R}}$ is the average variance for the track hits not in region R , that can be estimated using eq. 5 after excluding the hit in region R from the track. The estimator for σ_R^2 is thus

$$\begin{aligned} s_R^2 &= ns^2 - (n - 1)s_{\bar{R}}^2 = \\ &= n \frac{\sum_{i=1}^n (\bar{t} - t_i)^2}{(n - 1)} - (n - 1) \frac{\sum_{j \notin R}^{n-1} (\bar{t} - t_j)^2}{(n - 2)} = \\ &= \frac{1}{(n - 2)} \left[nt_R(t_R - 2\bar{t}) - \frac{\left(\sum_{i=1}^n t_i^2 - \left(\sum_{i=1}^n t_i \right)^2 \right)}{(n - 1)} \right] \end{aligned} \quad (7)$$

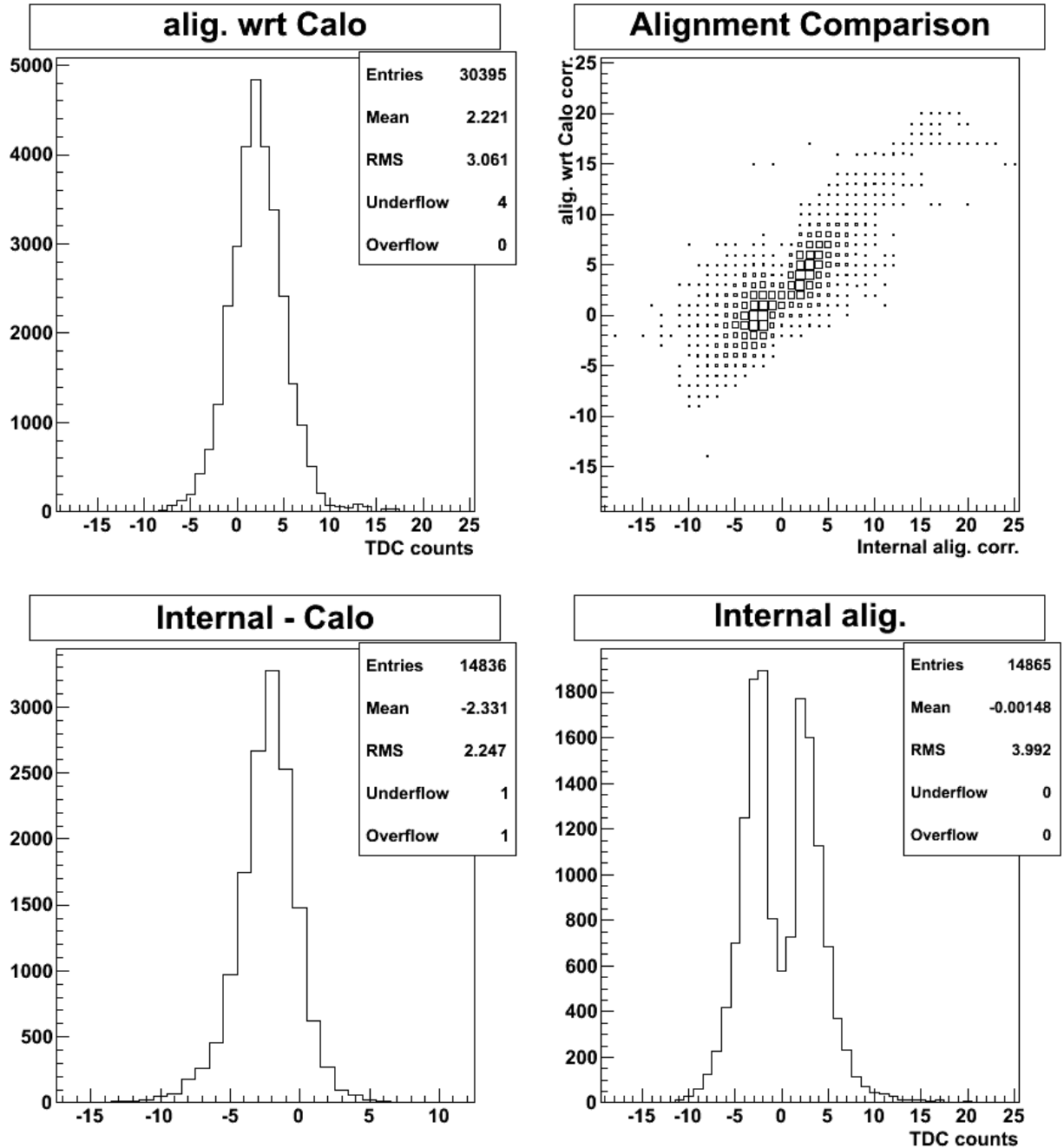


Figure 6 Comparison between the two sets of time shifts obtained using the internal alignment procedure and the alignment with respect to the calorimeter trigger. Shifts are expressed in TDC units (equivalent to 25/16 ns).

The method was validated using toy MonteCarlo, where different distributions were used to model the time response: gaussian, flat, and also taking the real shape measured on test stands. In all cases the results were compatible, within the statistical error, with the input value, proving that the method is unbiased and correctly implemented.

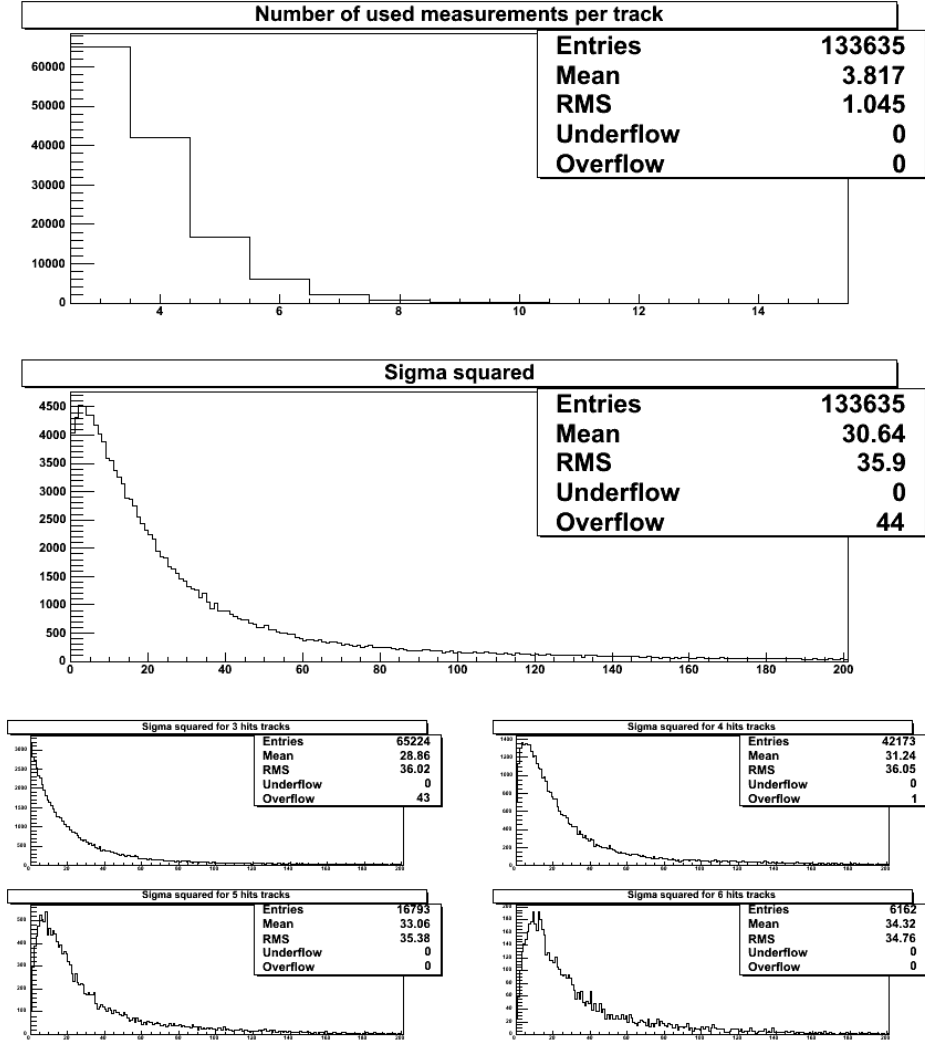


Figure 7 Distributions of number of time measurements per track n , and of s^2 for all tracks and for tracks with different n .

6.2 Results

We applied the method described in section 6.1 to estimate the resolution in each region. Quality cuts described in sections 2 and 4 and alignment corrections obtained with the procedure described in section 5.1 are applied. Assuming the same resolution for the same regions in station 2 and 3 and in stations 4 and 5, we end up with 10 unknown parameters, *i.e.* the resolutions for regions M23R1x, M23R1y, M23R2x, M23R2y, M23R3, M23R4, M45R1, M45R2, M45R3, M45R4.

Table 3 shows the results for all tracks and also grouping the tracks for different n values.

The value of the average variance corresponds to a resolution $\sigma = 6.04 \pm 0.01$ ns, in line with expectations for R4 chambers which dominate the sample.

Table 3 Results of resolution measurements, in ns. Errors are statistical only.

region	all	$n = 3$	$n = 4$	$n = 5$	$n = 6$
Average	6.04 ± 0.01	6.07 ± 0.02	6.00 ± 0.02	5.99 ± 0.03	6.00 ± 0.04
M23R1s	7.2 ± 0.1	7.1 ± 0.4	7.4 ± 0.2	7.2 ± 0.2	7.1 ± 0.2
M23R1p	6.4 ± 0.1	6.0 ± 0.3	6.5 ± 0.2	6.5 ± 0.2	6.6 ± 0.2
M23R2s	6.5 ± 0.1	6.7 ± 0.2	6.8 ± 0.1	6.6 ± 0.1	6.2 ± 0.1
M23R2p	7.1 ± 0.1	7.3 ± 0.2	7.2 ± 0.1	7.0 ± 0.1	7.0 ± 0.1
M23R3	5.8 ± 0.1	6.2 ± 0.1	5.7 ± 0.1	5.5 ± 0.1	5.3 ± 0.1
M23R4	5.7 ± 0.1	5.8 ± 0.1	5.7 ± 0.1	5.6 ± 0.1	5.5 ± 0.1
M45R1	7.8 ± 0.1	8.8 ± 0.5	8.0 ± 0.2	7.2 ± 0.3	7.0 ± 0.3
M45R2	6.2 ± 0.1	6.3 ± 0.1	6.1 ± 0.1	6.1 ± 0.1	6.3 ± 0.2
M45R3	6.4 ± 0.1	6.5 ± 0.1	6.4 ± 0.1	6.4 ± 0.1	6.4 ± 0.1
M45R4	6.1 ± 0.1	6.2 ± 0.1	6.0 ± 0.1	5.9 ± 0.1	5.5 ± 0.1

6.3 Systematics

As previously stated, a number of systematic effects limit the accuracy of this measurement. The non-linearity of the TDC mainly affects hits at the BX border. Removing the border TDC bins suppresses the effect but leads to a systematic underestimation of the resolution by limiting the range of the time measurement fluctuations. We evaluate this effect by comparing the results with:

- no cuts on TDC value (over-estimation of σ)
- removing hits in the last two bins (nominal analysis)
- removing hits in the last and first two bins (under-estimation of σ)

Results are shown on table 4. The effect on resolution is $\pm 0.5 - 1$ ns depending on the region. A residual effect with nominal cuts can be seen by comparing forward and backward tracks. Hits for forward tracks are more centered on the BX and are expected to be less affected by the TDC problem.

Table 4 Systematic study on the effect of TDC non-linearity. Results for σ in ns are reported for different cuts on the TDC range, and for forward and backward tracks separately.

region	Nominal cuts (remove bins 14 and 15)	no TDC cuts	remove bins 0, 1, 14, 15	only forward tracks	only backward tracks
Average	6.04 ± 0.01	6.83 ± 0.02	5.87 ± 0.01	5.87 ± 0.02	6.24 ± 0.02
M23R1x	7.2 ± 0.1	9.0 ± 0.1	6.9 ± 0.1	7.2 ± 0.2	7.3 ± 0.2
M23R1y	6.4 ± 0.1	8.1 ± 0.1	6.2 ± 0.1	6.4 ± 0.1	6.4 ± 0.2
M23R2x	6.5 ± 0.1	8.5 ± 0.1	6.2 ± 0.1	6.5 ± 0.1	6.5 ± 0.1
M23R2y	7.1 ± 0.1	8.6 ± 0.1	6.8 ± 0.1	7.0 ± 0.1	7.4 ± 0.1
M23R3	5.8 ± 0.1	6.3 ± 0.1	5.9 ± 0.1	5.6 ± 0.1	6.0 ± 0.1
M23R4	5.7 ± 0.1	6.4 ± 0.1	5.6 ± 0.1	5.5 ± 0.1	5.9 ± 0.1
M45R1	7.8 ± 0.1	9.7 ± 0.2	7.4 ± 0.2	7.9 ± 0.2	7.7 ± 0.2
M45R2	6.2 ± 0.1	6.8 ± 0.1	6.0 ± 0.1	5.9 ± 0.1	6.5 ± 0.1
M45R3	6.4 ± 0.1	7.2 ± 0.1	6.2 ± 0.1	6.3 ± 0.1	6.5 ± 0.1
M45R4	6.1 ± 0.1	6.5 ± 0.1	5.8 ± 0.1	5.7 ± 0.1	6.4 ± 0.1

As shown in sec. 5, the contribution of residual time misalignment to the resolution is expected to be sizeable. Table 5 shows the comparison of results without alignment corrections and with the two sets of corrections described in sec. 5.1 and 5.2. The effect on the average resolution is $\sqrt{(\sigma^2)_{noalign} - (\sigma^2)_{align}} = 4.8$ ns, in agreement

with what anticipated in section 5.

As discussed there, using the internal procedure we expect a residual systematic overestimation of σ in inner regions due to the limited statistics, and a small underestimation due to overtraining. The latter is due to the difference between the real average residual of each channel and the measured value on the same data sample of the resolution measurement. To estimate this bias, we repeated the analysis after adding to each alignment constant a random quantity generated according to a gaussian with σ equal to the statistical error of the average residual. The effect on the resolution is <0.2 ns in all regions.

For the second alignment procedure using calorimeter, we expect a systematic overestimation due to the grouping procedure and to the calorimeter misalignment.

Table 5 Effect of time alignment. Results for σ in ns are reported with and without time alignment corrections.

region	No time alignment	using internal alignment	using internal align. + random spread	using alignment with calorimeters
Average	7.69 ± 0.01	6.04 ± 0.01	6.12 ± 0.01	6.32 ± 0.01
M23R1x	8.7 ± 0.1	7.2 ± 0.1	7.4 ± 0.1	8.2 ± 0.1
M23R1y	8.3 ± 0.1	6.4 ± 0.1	6.6 ± 0.1	7.2 ± 0.1
M23R2x	9.0 ± 0.1	6.5 ± 0.1	6.7 ± 0.1	7.2 ± 0.1
M23R2y	9.4 ± 0.1	7.1 ± 0.1	7.2 ± 0.1	7.5 ± 0.1
M23R3	7.0 ± 0.1	5.8 ± 0.1	5.9 ± 0.1	6.2 ± 0.1
M23R4	7.4 ± 0.1	5.7 ± 0.1	5.8 ± 0.1	5.9 ± 0.1
M45R1	9.1 ± 0.2	7.8 ± 0.2	8.0 ± 0.2	8.7 ± 0.2
M45R2	7.4 ± 0.1	6.2 ± 0.1	6.3 ± 0.1	6.8 ± 0.1
M45R3	7.7 ± 0.1	6.4 ± 0.1	6.5 ± 0.1	6.7 ± 0.1
M45R4	7.8 ± 0.1	6.1 ± 0.1	6.1 ± 0.1	6.2 ± 0.1

Another cross-check consists in using a subsample of the data (about 2/3 of statistics from the first two nights of data) for computing the alignment corrections, and the remaining data (the third night) for computing the resolution. This avoids the effect of overtraining, but the decrease of statistics is critical for the internal alignment procedure (channels with a significant correction decrease by 40% in R1 region). For the second procedure using grouping, the decreased statistics is less critical and the effect on the measured resolution is much smaller. Results are shown on table 6.

Table 6 Resolution measured from the third night, using the first two for computing the alignment.

region	No time alignment	using internal alignment	using alignment with calorimeters
M23R1x	9.1 ± 0.2	9.1 ± 0.2	8.5 ± 0.2
M23R1y	8.5 ± 0.2	8.2 ± 0.2	7.6 ± 0.2
M23R2x	8.8 ± 0.1	7.4 ± 0.1	7.1 ± 0.1
M23R2y	9.3 ± 0.1	7.4 ± 0.1	7.5 ± 0.1
M23R3	7.2 ± 0.1	6.7 ± 0.1	6.6 ± 0.1
M23R4	7.5 ± 0.1	6.0 ± 0.1	6.0 ± 0.1
M45R1	9.2 ± 0.3	9.1 ± 0.3	8.8 ± 0.3
M45R2	7.2 ± 0.1	7.0 ± 0.1	6.8 ± 0.1
M45R3	7.7 ± 0.1	6.6 ± 0.1	6.7 ± 0.1
M45R4	7.7 ± 0.1	6.1 ± 0.1	6.2 ± 0.1

The presence of ghost hits is another possible source of systematic error. We evaluate it by removing the cut on the time difference between the two views on crossed pads. The typical effect is an increase of σ by 0.3 ns, as shown on table 7. This is a conservative estimate, since the TDC non-linearity also contributes to the tails of the time difference. As a further cross-check, we compare the results using tracks crossing three or four stations.

Finally, we look at the result as a function of the cluster size in order to spot the possible contribution of cross-talk, expected to spoil the resolution for large cluster size, and of signal amplitude effects that should produce

Table 7 Results for σ in ns are reported after releasing the Δt cut, and selecting tracks crossing three or four stations.

region	nominal analysis	release Δt cut	crossing 3 stations	crossing 4 stations
M23R1x	7.2 ± 0.1	7.7 ± 0.1	7.3 ± 0.1	7.2 ± 0.2
M23R1y	6.4 ± 0.1	6.7 ± 0.1	6.5 ± 0.1	6.2 ± 0.2
M23R2x	6.5 ± 0.1	6.9 ± 0.1	6.6 ± 0.1	6.4 ± 0.1
M23R2y	7.1 ± 0.1	7.5 ± 0.1	7.2 ± 0.1	7.0 ± 0.1
M23R3	5.8 ± 0.1	6.4 ± 0.1	5.9 ± 0.1	5.6 ± 0.1
M23R4	5.7 ± 0.1	6.0 ± 0.1	5.7 ± 0.1	5.7 ± 0.1
M45R1	7.8 ± 0.2	8.0 ± 0.2	7.9 ± 0.2	7.6 ± 0.3
M45R2	6.2 ± 0.1	6.7 ± 0.1	6.2 ± 0.1	6.0 ± 0.1
M45R3	6.4 ± 0.1	6.7 ± 0.1	6.4 ± 0.1	6.4 ± 0.1
M45R4	6.1 ± 0.1	6.2 ± 0.1	6.1 ± 0.1	6.0 ± 0.1

an opposite bias (larger cluster size correspond to larger signal amplitude that should have better resolution, especially with the high thresholds used). Results, displayed on table 8, show no significant biases.

Table 8 Results for σ in ns for different cluster size.

region	all	cs=1	cs=2	cs=3	cs=4
M23R1s	7.2 ± 0.1	7.3 ± 0.1	7.1 ± 0.2	7.4 ± 0.5	5.7 ± 0.6
M23R1p	6.4 ± 0.1	6.4 ± 0.1	6.5 ± 0.2	6.3 ± 0.6	6.5 ± 0.7
M23R2s	6.5 ± 0.1	6.8 ± 0.1	6.1 ± 0.1	6.4 ± 0.2	6.1 ± 0.4
M23R2p	7.1 ± 0.1	7.2 ± 0.1	7.0 ± 0.1	7.7 ± 0.2	6.9 ± 0.4
M23R3	5.8 ± 0.1	6.1 ± 0.1	5.4 ± 0.1	5.1 ± 0.1	6.1 ± 0.5
M23R4	5.7 ± 0.1	5.8 ± 0.1	5.5 ± 0.1	5.4 ± 0.1	5.8 ± 0.5
M45R1	7.8 ± 0.1	8.1 ± 0.2	6.9 ± 0.2	8.2 ± 0.6	-
M45R2	6.2 ± 0.1	6.2 ± 0.1	6.1 ± 0.1	6.0 ± 0.3	5.6 ± 0.7
M45R3	6.4 ± 0.1	6.5 ± 0.1	6.2 ± 0.1	6.5 ± 0.2	8.0 ± 1.4
M45R4	6.1 ± 0.1	6.3 ± 0.1	5.5 ± 0.1	5.7 ± 0.1	-

7 Conclusions

We can summarize the findings of this analysis with the following:

- Our sample of 1.4M calorimeter cosmic trigger allows to refine the detector time alignment to a satisfactory level for regions 3 and 4. The alignment is still limited by statistics for regions 1 and 2. By acquiring a sample ten times larger, all channels could be aligned with an accuracy better than 2 ns;
- the resolution can be estimated simultaneously for all regions without the need for other detectors;
- resolutions values between 5.5 and 7.5 ns are measured, showing that the detector performance is under control;
- the resolution measurement is limited by systematic effects, mostly due to the TDC non-linearity and by the limited statistics of the alignment procedure.

For the total systematic error on the resolution for each region we quote half of the spread of the results for the different systematic checks of sec. 6.3. In table 9 we compare these values with the predictions of sec. 3. The results agree within the uncertainty.

The 2008 cosmic sample proved to be very useful to understand and debug the detector, and provide a first assessment of its performance. More cosmic data to be taken during the 2009 commissioning, with nominal HV and threshold conditions and a much smaller number of problematic channels, will allow to improve the accuracy of this analysis and to provide an estimate of the muon detector efficiency in the 25 ns time window.

Table 9 Comparison between the measured values of the resolution (in ns) at the pit and the expected values from laboratory tests. Errors are dominated by systematics.

region	Measured	Expected
M23R1x	7.2 ± 1.5	5.2 ± 1.0
M23R1y	6.4 ± 1.0	
M23R2x	6.5 ± 1.1	
M23R2y	7.1 ± 0.9	
M23R3	5.8 ± 0.6	
M23R4	5.7 ± 0.5	5.5 ± 1.0
M45R1	7.8 ± 0.6	
M45R2	6.2 ± 0.4	
M45R3	6.4 ± 0.5	
M45R4	6.1 ± 0.5	

8 References

- [1] LHCb Collaboration, *LHCb muon system technical design report*, CERN-LHCC-2001-010
- [2] G. Passaleva, *A recurrent neural network for track reconstruction in the LHCb Muon System*, Nuclear Science Symposium Conference Record, NSS '08 IEEE, pp.867-872 (2008)
- [3] E. Furfaro, G. Martellotti, R. Nobrega, G. Penso and D. Pinci, *Study of the LHCb muon chambers performance with cosmic rays* J. Phys. Conf. Ser. **110** (2008) 122017
- [4] A. Alves *et al.*, *Gas gain uniformity tests performed on multi wire proportional chambers for the LHCb muon system*, Nucl. Instrum. Meth. A **591** (2008) 374
- [5] M. Frosini and G. Passaleva, "Measurement of the time alignment between muon detector and calorimeters with the 2008 cosmic runs", public LHCb note in preparation
- [6] W. Bonivento and G. Manca, *Measurement of the logical pad cluster size of the installed muon chambers with the 2008 cosmic runs*, LHCb Public Note, LHCb-2009-031
<http://cdsweb.cern.ch/record/1163365/files/LHCb-2009-031.pdf>